REAL-TIME MONITORING OF DAMAGE DEVELOPMENT IN CROSSPLY COMPOSITE LAMINATES BY MEANS OF ULTRASONIC AND ACOUSTIC EMISSION METHODS

Shi-Chang Wooh
Department of Civil and Environmental Engineering
Massachusetts Institute of Technology
Cambridge, Massachusetts 02139

Isaac M. Daniel and Heoung-Jae Chun
Robert R. McCormick School of Engineering and Applied Science
Northwestern University, Evanston, Illinois 60208

INTRODUCTION

Studies on damage development in composite laminates have been conducted by many investigators [1-3]. In the case of crossply laminates under uniaxial tensile loading, whether monotonic or cyclic, the first stage of damage consists of transverse matrix cracking in the 90° plies. These cracks are nearly equidistant and increase in density up to a characteristic limiting value. In the later stages of loading, the damage evolves so that longitudinal cracks are generated in the 0° plies, followed by micro-delaminations at the intersections of the two sets of cracks, and finally fiber failures leading to global failure [1].

As the damage evolves, material properties are degraded. In particular, stiffness degradation due to matrix cracking is a significant indication of damage [4-6] and the measurement of matrix crack density is important in the prediction of residual life. It is often desirable to evaluate such damage in the material nondestructively.

In this study, a real time nondestructive evaluation method was developed and applied to detection of damage evolution in composite materials for the purpose of developing damage accumulation and life prediction models. An attempt was made in an effort to characterize the damage and to correlate the ultrasonic backscattered energy and acoustic emission readings with damage in real time.

EXPERIMENTAL PROCEDURE

The material used was IM7/8551-A (Hercules) graphite/epoxy received in prepreg form. It was fabricated into coupons of $[0/90_4]_s$ crossply layup for mechanical and

Review of Progress in Quantitative Nondestructive Evaluation, Vol. 14
Edited by D.O. Thompson and D.E. Chimenti, Plenum Press, New York, 1995

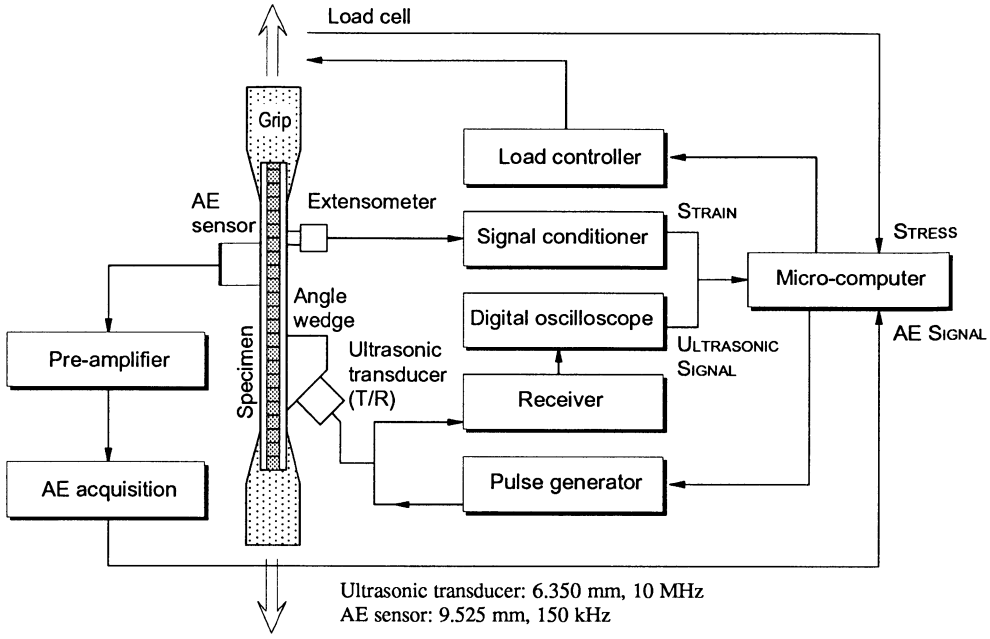

Fig. 1. Schematic diagram of system used for real-time monitoring of damage in composite materials.

nondestructive testing. The specimen was loaded in a servo-hydraulic tensile testing machine controlled by a host micro-computer while the damage was monitored by ultrasonic and acoustic emission (AE) methods. Figure 1 shows schematically the setup used in this study.

An unfocused ultrasonic transducer of 10 MHz center frequency was mounted on the surface of the specimen. The transducer operating in pulse echo mode sends repetitive ultrasonic pulses onto the specimen at an oblique angle perpendicular to the inner 90° layer guided by the angle wedge [7]. The propagating ultrasonic beam is then scattered back to the transducer from the crack tips or other small flaws. The signals were recorded by a 200 MHz digital oscilloscope and transferred to the host computer for numerical processing. The computed backscattered energy of the signal was correlated with the corresponding stress-strain curve.

The acoustic emission (AE) sensor (9.525 mm dia., 150 kHz center frequency) was mounted in contact with the specimen. The AE output was independently recorded by the AE acquisition system (Locan-AT, Physical Acoustics). Since the frequency bands of the ultrasonic transducer and the AE sensor are different and far apart (10 MHz vs. 150 kHz center frequency), there was no interference between the signals. However, the repetition rate of the ultrasonic pulses may interfere with the AE signals so that proper setting of the pulse repetition rate was needed.

In addition to ultrasonic and AE measurements, the matrix crack density was independently measured by the edge replication method at the corresponding stress levels. The edge replication technique is advantageous over X-radiography because there is no need to unload the specimen. The specimen edge was prepared with quickly evaporating acetone.

The edge was then replicated by a thin replication tape (Ernest Fullam) before the acetone evaporated. This procedure can be done within seconds during a brief pause in testing.

Several AE parameters were investigated in this study: amplitude, counts, and events. It is necessary to find the characteristics of the signals from various sources of AE in order to identify failure mechanisms. For example, the signals due to friction from inside the material should be distinguished from the signals due to matrix cracking. For this purpose, the AE amplitude and count-frequency of the AE events were displayed in terms of corresponding strain levels.

RESULTS AND DISCUSSION

Figure 2 shows a typical stress-strain curve and the measured crack density for a $[0/90_4]_s$ laminate. The initial region of the stress-strain curve (A–B) corresponds to the linear elastic behavior of the laminate where no macroscopic damage was found. It is noted from the curve that the stress-strain curve deviates from the linear behavior immediately after the first generation of transverse matrix cracks are observed (Point B). As the load increases, the crack density increases at a constant rate. As a result, the tangential modulus of the material in this range is lower than the initial modulus. When the stress level reaches point C, the cracking is stabilized or the rate slows down. Above this level, in region C–D, different failure mechanisms such as longitudinal matrix cracking, micro-delaminations, and fiber fractures take place. Eventually the material fails globally.

Figure 3 shows the stress-strain curve and the measured backscattered energy for the $[0/90_4]_s$ laminate. There exist some background scatter signals even for the virgin specimen. This initial energy level represents surface roughness and material inhomogeneity. As long as the specimen-transducer contact condition remains constant, this quantity remains constant for the entire loading period. Thus, the backscattered energy was normalized by the initial value at the unstressed stage.

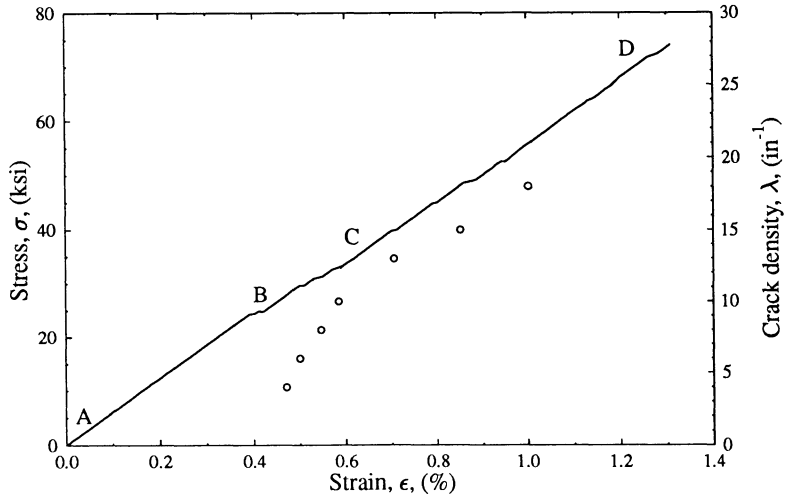

Fig. 2. Stress-strain curve and transverse crack density as a function of applied strain for $[0/90_4]_s$ IM7/8551-7A graphite/epoxy laminate.

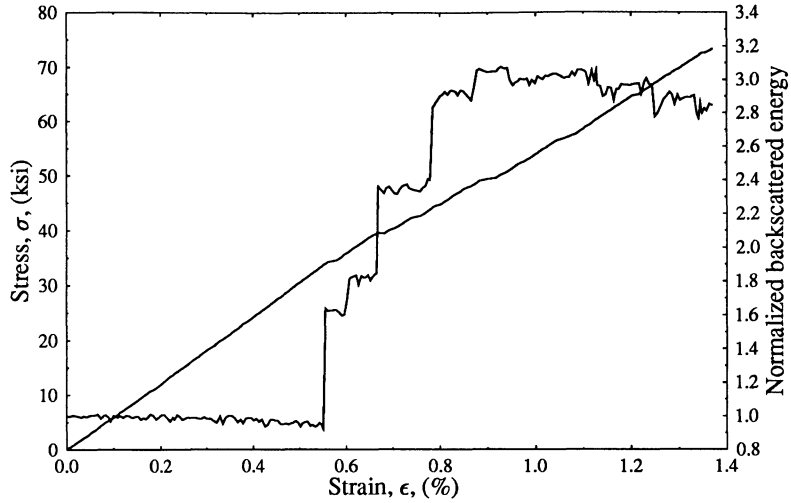

Fig. 3. Stress-strain curve and ultrasonic backscattered energy as a function of applied strain for $[0/90_4]_s$ IM7/8551-7A graphite/epoxy laminate.

In the linear elastic range of the stress-strain curve, virtually no damage is found and the backscattered energy is constant. When the first macrocracks appear at approximately 0.575% strain, the stress-strain curve deviates slightly from linearity. In this matrix cracking region, the backscattered energy increases sharply in steps up to the point where cracking stabilizes. It should be noted that there is some uncertainty in the detection of the first generation of cracks particularly when the size of the transducer is smaller than the average crack spacing. In our case, the diameter of the transducer was 6.35 mm (0.25 in.) and the minimum detectable crack density was 0.157 mm^{-1} (4 in^{-1}) as shown in Fig. 2.

At the crack stabilizing point, the backscattered energy is stabilized or starts decreasing whereas the stress-strain curve becomes linear. In this region, damage appears in the outer zero degree layers. Longitudinal cracks and micro-delaminations as well as fiber fractures in these layers cause the ultrasound to scatter in different directions. Therefore, a lower amount of ultrasonic energy is propagated into the inner layer where matrix cracks exist, resulting in lower backscattered energy returned to the transducer.

Besides ultrasonic scattering, acoustic emission output was recorded. First, the amplitude of the AE events was studied. Figure 4 shows a histogram or the probability density function (PDF) of AE events as a function of amplitude during the entire monotonic loading period. As shown in the figure, the distribution of the histogram is bipolar. This means that there are numerous signals of small amplitude as well as a large number of high amplitude but relatively fewer medium amplitude signals. This presentation of the histogram, however, provides no correlation of AE events with failure mechanisms.

The histogram should be interpreted in conjunction with the corresponding stress-strain behavior (Fig. 2). Figure 5 alternatively shows histograms of AE events for various amplitude ranges as a function of applied strain. Alternatively, the histogram is plotted as a function of both amplitude and strain in the form of a three-dimensional plot as shown in Fig. 6(a). Both plots show that AE events of high amplitude (> 85 dB) dominate in the range of strains between points B and C where matrix cracking is predominant. Numerous low amplitude signals appear in region C–D. This leads to the conclusion that the amplitude of

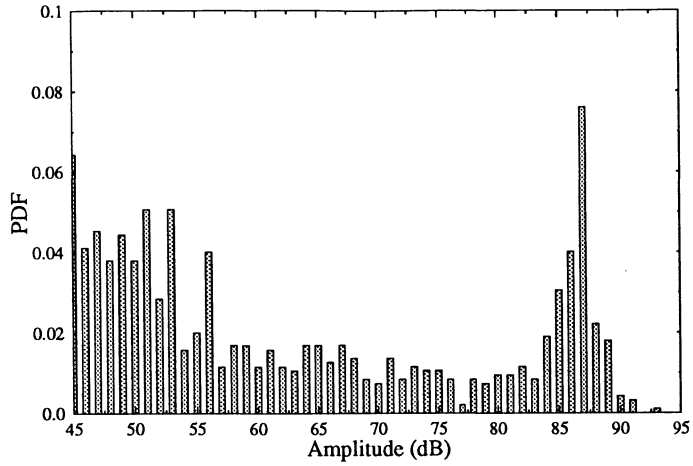

Fig. 4. Histogram of AE events as a function of amplitude for $[0/90_4]_s$ IM7/8551-7A graphite/epoxy laminate.

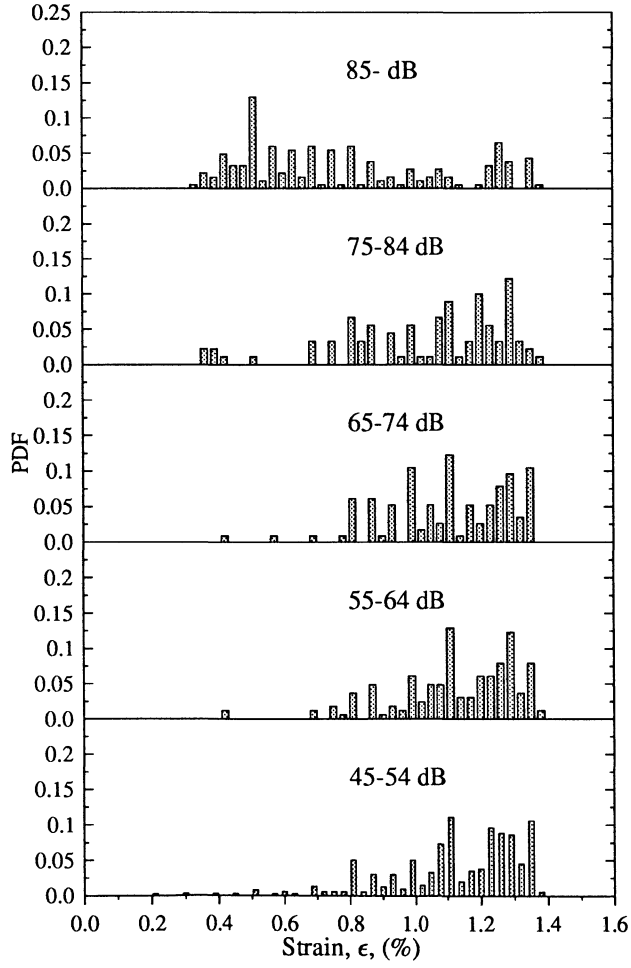

Fig. 5. Histogram of AE events for various amplitude ranges as a function of strain for $[0/90_4]_s$ IM7/8551-7A graphite/epoxy laminate.

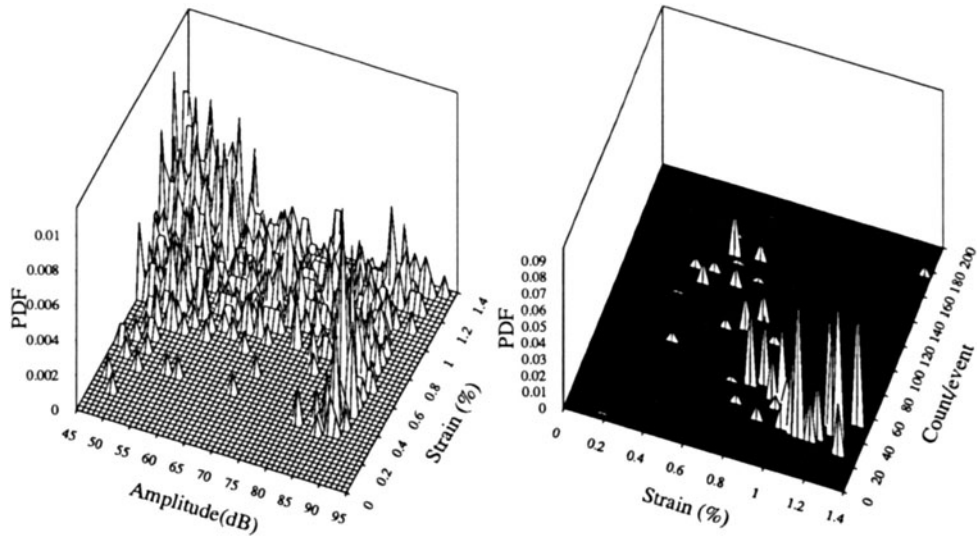

Fig. 6. Distribution of AE events as a function of (a) strain and amplitude, (b) strain count frequency for $[0/90_4]_s$ IM7/8551-7A graphite/epoxy laminate.

the AE signals from matrix cracking is the highest. As the strain increases, there are numerous low amplitude signals (between 45 to 54 dB). These signals appear after most of the cracking is finished so that it is believed that these signals are due to frictional noise at the cracks and other damage. Also noted is a peak of high amplitudes at high strains near ultimate failure of the material, that is the stage of fiber bundle fractures. Fiber fractures generate AE signals of amplitude as high as those of matrix cracking.

Frequency distribution of the AE signal is another useful feature. The frequency content is obtained from the AE signal by Fourier analysis. However, for convenience, the number of counts per event (count frequency), which represents approximately the frequency of the signal, was used in this study. Figure 6(b) shows a three-dimensional plot of the distribution of AE events as a function of strain and count frequency. Most of the low frequency signals are the noise which occurs in the strain range between 0.7 to 1.3 %. Several peaks are found in the matrix cracking region or the count frequency range of 80–160. Also note that there is a small peak near global failure corresponding to failure of fiber bundles. From these facts, we conclude that the signals from matrix cracking and fiber bundle fractures are high in both amplitude and frequency.

AE was also monitored continuously during loading/unloading tests. Figure 7 shows the stress and cumulative AE counts as a function of applied strain. The slope of the envelope of the cumulative AE counts shows the rate of AE output. No AE events are produced in the linear range below 0.4 % strain. The slope of the envelope is the highest in the matrix cracking region and slows down above the point where cracking stabilizes.

The envelope of the loading/unloading stress-strain curve matches the monotonic stress-strain curve. This implies that the loading/unloading process produces no significant additional damage in the material. During reloading very few additional AE events are detected. This confirms the Kaiser effect.

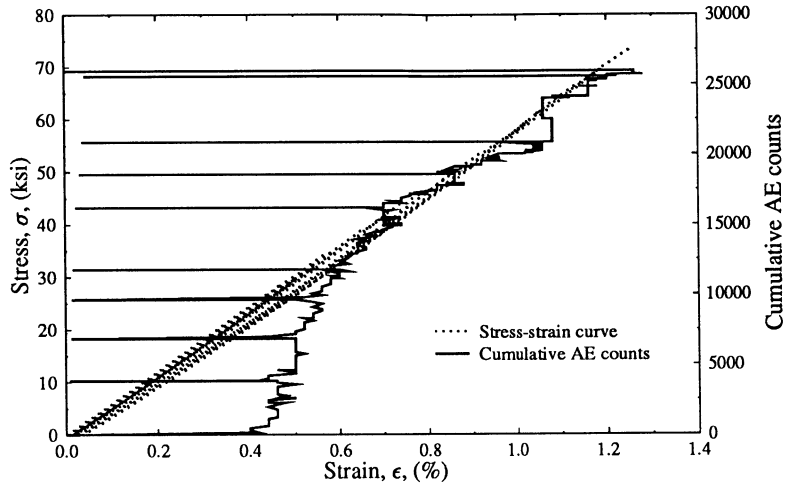

Fig. 7. Stress and cumulative counts versus strain for loading and unloading of $[0/90_4]_s$ IM7/8551-7A graphite/epoxy laminate.

SUMMARY AND CONCLUSIONS

Progressive failure mechanisms of a crossply composite laminate under uniaxial tension was characterized by correlating the ultrasonic and acoustic emission readings with damage in real time. Both ultrasonic backscattered energy and acoustic emission gave consistent results and are proved to be sensitive indicators of matrix cracking and other failure mechanisms. An attempt was made to extract the signatures of the AE signals by investigating the amplitude and count frequency. Loading/unloading tests showed that no additional damage occurs upon reloading up to the previous peak loading.

Matrix cracking was correlated with the associated ultrasonic backscattered energy and acoustic emission output. The stiffness degradation of the material due to matrix cracking could be used in the correlation with ultrasonic measurements. Both parameters gave consistent results.

Ultrasonic backscattered energy is constant in the linear region of the stress-strain curve. In this region no acoustic emission events were detected.

In the matrix cracking region, matrix crack density increases quickly and the backscattered energy increases sharply in steps corresponding to stiffness degradation. In this region, numerous AE signals of high amplitude and high frequency are detected.

As the cracking and stiffness are stabilized, the backscattered energy is stabilized or starts decreasing whereas the stress-strain behavior becomes linear. High amplitude acoustic emission signals are reduced in this region but numerous AE signals of low amplitude, low frequency noise are produced. Isolated high amplitude AE signals are noticed in the last part of the stress-strain curve, possibly associated with other failure mechanisms.

A series of loading and unloading tests were conducted. Both backscattered energy and AE measurements during loading/unloading tests showed that no additional damage occurs upon reloading up to the previous peak loading (Kaiser effect).

ACKNOWLEDGEMENT

This work was sponsored by the Air Force Office of Scientific Research (AFOSR). The authors are grateful to Dr. Walter Jones of AFOSR for his encouragement and cooperation.

REFERENCES

1. A. Charewicz and I. M. Daniel, "Damage mechanisms and accumulation in graphite/epoxy laminates," *Composite Materials: Fatigue and Fracture*, ASTM STP 907, ed. H. T. Hahn, ASTM, Philadelphia, 1986, 274–297.
2. I. M. Daniel and J.-W. Lee, "Damage development in composite laminates under monotonic loading," *J. Composites Technology and Research* **12**(2), 1990, 98–102.
3. I. M. Daniel, S. C. Wooh, and J. W. Lee, "Nondestructive Evaluation of Damage Development in Composite Materials," *Elastic Waves and Ultrasonic Nondestructive Evaluation*, S. K. Datta, J. D. Achenbach, and Y. S. Rajapakse eds., Elsevier, 1990, 183–189.
4. R. Talreja, "Transverse cracking and stiffness reduction in composite laminates," *J. Comp. Mat.* **19**, 1985, 355–375.
5. S. L. Ogin, P. A. Smith, and P. W. R. Beaumont, "Matrix cracking and stiffness reduction during the fatigue of a $[0/90_2]_s$ GFRP laminate," *Composites Science and Technology* **22**, 1985, 23–31.
6. C.-L. Tsai, and I. M. Daniel, "The behavior of cracked crossply composite laminates under general in-plane loading," *Damage in Composite Materials*, ed. G. Z. Voyiadjis, Elsevier, 1993, 51–66.
7. S. C. Wooh and I. M. Daniel, " Real-time ultrasonic monitoring of fiber-matrix debonding in ceramic-matrix composite," *Mechanics of Materials* **17**, 1994, 379–388.